

Ultrafast Coherent Interactions in Quantum Wells Studied by Two-Dimensional Fourier Transform Spectroscopy

Tianhao Zhang,¹ Irina Kuznetsova,² Lijun Yang,³ Alan D. Bristow,¹ Xingcan Dai,¹ Xiaoqin Li,⁴ Torsten Meier,⁵ Peter Thomas,² Shaul Mukamel,³ Richard P. Mirin⁶ and Steven T. Cundiff¹

¹JILA, University of Colorado and National Institute of Standard and Technology, Boulder, CO 80309-0440 U.S.A.

²Department of Physics and Material Sciences Center, Philipps University, Renthof 5, D-35032 Marburg, Germany

³Department of Chemistry, University of California, Irvine, CA 92697-2025 U.S.A.

⁴Department of Physics, University of Texas, Austin, TX 78712-0264 U.S.A.

⁵Department Physik, Fakultät für Naturwissenschaften, Universität Paderborn, Warburger Strasse 100, D-33098 Paderborn, Germany

⁶National Institute of Standards and Technology, Boulder, CO 80305 U.S.A.

E-mail: cundiffs@jila.colorado.edu

Abstract. Many-body effects dominate the polarization studies of heavy- and light-hole excitons. Accurate simulations require Coulomb correlations beyond Hartree-Fock approximation. Raman coherences are isolated with a new two-dimensional projection.

Coherent excitation of carriers has been studied extensively by transient four-wave mixing (TFWM) spectroscopy. While versatile, this technique has several limitations. Developed from TFWM, two-dimensional Fourier-transform (2DFT) spectroscopy^{1,2} is the optical analogue of multi-dimensional nuclear magnetic resonance spectroscopy. Multi-dimensional techniques unfold coherent peaks associated with populations (diagonal features) from coherent coupling between states (off-diagonal features), typically by plotting the signal versus both the absorption and emission photon energies. The advantage of this technique is that it can clearly separate a) self-coherent peaks from cross-coherent peaks, b) quantum beats from polarization beats, c) different many-body interactions,^{3,4,5} and d) homogeneous from inhomogeneous broadening.⁶

2DFT spectroscopy has recently become a rigorous experimental test for many-body interactions of semiconductor excitons, in particular the heavy- and light-hole coherences. (See Fig 1 (a) for a typical absorption spectrum.) 2DFT spectroscopy has pushed the theoretical modelling to the level of many-body correlations that include all excitonic and biexcitonic contributions. These solutions go beyond phenomenological approaches of many-body effects,⁶ such as excitation-induced dephasing and shift or local-field corrections.

The similarity of 2DFT spectroscopy to other techniques like multi-dimensional NMR provides a wealth of expertise applicable to the spectroscopy of semiconductors. For example, the use of different two-dimensional (2D) projections allows for the separation of otherwise co-contributing Feynman pathways within the heavy- and light-hole system.⁷ Separation of these pathways can also be modelled with a microscopic many-body theory based on the semiconductor Bloch equations.

Our experimental setup (described in detail in ref. [2]) uses heterodyne detection of the spectrally resolved TFWM signal over a range of time delays. A Fourier transform produces a 2D map that represents the section of the density matrix allowed by the specified geometry and time ordering of the pulses. A three-pulse box geometry is used, where the signal is detected in the $-k_A+k_B+k_C$ direction and scanning pulse A provides rephasing (photon-echo) information.

The non-rephasing information is similarly obtained by scanning pulse B . In this standard $S_I(\omega_r, T, \omega_i)$ experiment the 2D map is equivalent to a plot of the absorption versus emission photon energies. Alternatively, the time delay between pulses B and C can be scanned, yielding a 2D map of the mixing versus emission photon energies, denoted $S_I(\tau, \omega_r, \omega_i)$.

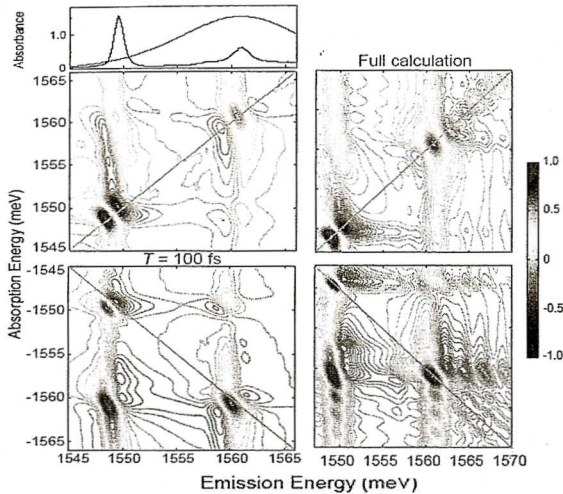


Fig.1 (a) Absorbance spectrum of the HH and LH excitons. Real-part of the $S_I(\omega_r, T, \omega_i)$ 2DFT spectra for co-circular excitation in the (b) non-rephasing and (c) rephasing configurations. Theoretical comparison: (d) to (b) and (e) to (c).

The samples are grown by molecular beam epitaxy, consisting of 10⁴ period GaAs/AlGaAs multiple quantum wells, with 10 nm wells and barriers. The samples are attached to wedged sapphire disks and the substrate is removed by lapping and etching. Measurements are performed at temperatures below 10 K.

Numerical simulations are based on a one-dimensional tight-binding model. The microscopic semiconductor Bloch equations include exciton and biexciton formation and Coulomb correlations due to exciton-exciton and exciton-biexciton interaction; further details are given in ref. 6 and 7.

The interplay of heavy- and light-hole excitons is examined for a variety of polarizations, using the real-part of the $S_I(\omega_r, T, \omega_i)$ projections. Experimental rephasing and non-rephasing spectra are shown in Fig. 1 (b) and (c), with the associated theoretical plots in (d) and (e). The diagonal features have dispersive line shapes, that appear as derivatives of the TFWM pulse in the cross-diagonal direction for the rephasing and the diagonal direction for the non-rephasing. Simple models give absorptive line shapes, but the introduction many-body interactions (even at the Hartree-Fock level) give dispersive shapes too. Indeed from previous work this effect appears to be dominated by excitation-induced shifts.³ Compared to co-linear polarized excitation (not shown), co-circular excitation is expected to decouple the HH and LH exciton resonances due to selection rules, if many-body correlations and valence band-mixing effects are neglected. The full simulation exhibits the non-diagonal peaks seen in the experiment for the co-circular case. Thus they can be explained by many-particle correlations within the $\chi^{(3)}$ limit. Neglecting these higher-order terms leads to poor comparison to the experimental data; see ref. 4 for further comparison.

Amplitude $S_I(\tau, \omega_r, \omega_i)$ spectra are shown in Fig. 2 (a). This projection can isolate the so-called Raman coherences⁷ that contribute to the cross peaks in $S_I(\omega_r, T, \omega_i)$ spectra. Raman coherences correspond to Feynman pathways that oscillate with the mixing time T , and are normally obscured by stronger non-oscillating pathways. In the $S_I(\tau, \omega_r, \omega_i)$ spectra, the latter collapse into the zero-energy peaks along the center of the plot, thus exposing the Raman coherences. The overwhelming amplitude of the non-oscillating coherences is one reason why

the zero-energy peaks saturate this figure. An asymmetry is observed in the amplitude of the HH-LH and LH-HH Raman coherences [peaks indicated in Fig.2 (b)]. This is most likely due to their respective dephasing rates and the overlap of the heavy-hole continuum with the light-hole exciton. The experimental data is well reproduced by the microscopic many-body theory, as shown in Fig. 2 (b). Calculations are performed in the coherent limit and exciton dephasing rates are estimated from $S_I(\omega_r, T, \omega_e)$ experiments.

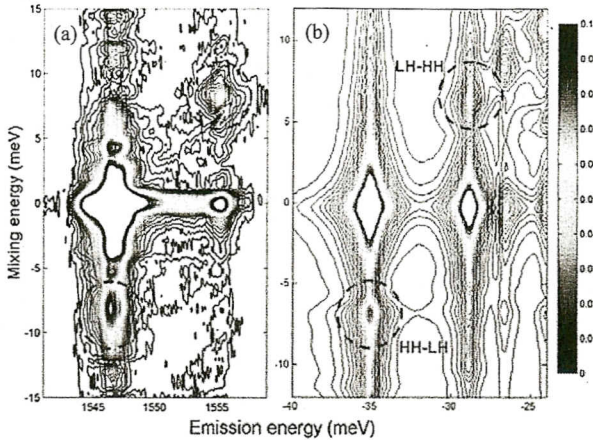


Fig.2 (a) Experimental and (b) theoretical amplitude of the $S_I(\tau, \omega_r, \omega_e)$ 2DFT spectra for co-linear excitation. The dashed circles show the excitonic Raman coherences.

It would also be interesting to investigate the real-part of the $S_I(\tau, \omega_r, \omega_e)$ spectra. This requires all three pump pulses in the box geometry be phase-locked. Apparatus is being presently built to perform these types of measurements. Additionally, the new apparatus would allow for examination of two-quantum transitions in biexcitons.⁸

Two-dimensional Fourier-transform spectroscopy has been applied to exciton dynamics in semiconductor quantum wells. It clearly reveals the dominance of many-body interactions that are accurately modeled by the semiconductor Bloch equations that include all exciton and biexciton Coulomb correlations within the $\chi^{(3)}$ limit. The experiments have been performed for various polarizations, time ordering and 2D projections. Both $S_I(\omega_r, T, \omega_e)$ and $S_I(\tau, \omega_r, \omega_e)$ projections demonstrate that two-dimensional Fourier-transform spectroscopy is presently the most stringent tool for many-body interactions in semiconductors. Also, the future application of the $S_I(\tau, \omega_r, \omega_e)$ projection may yield useful information about other systems, such as photosynthetic complexes,⁹ which have been studied with the $S_I(\omega_r, T, \omega_e)$ projection.

- 1 C. N. Borca, T. Zhang, X. Li and S. T. Cundiff, *Chem. Phys. Lett.* **416**, 311 (2005).
- 2 T. Zhang, C. N. Borca, X. Li and S. T. Cundiff, *Opt. Exp.* **13**, 7432-7441 (2005).
- 3 X. Li, T. Zhang, C. N. Borca, and S. T. Cundiff, *Phys. Rev. Lett.* **96**, 057406 (2006).
- 4 T. Zhang, I. Kuznetsova, T. Meier, X. Li, R. P. Mirin, P. Thomas and S. T. Cundiff, *Proc. Natl. Sci. USA* **104**, 14227 (2007).
- 5 I. Kuznetsova, P. Thomas, T. Meier, T. Zhang, X. Li, R. P. Mirin, and S. T. Cundiff, *Solid State Commun.* **142**, 154 (2007).
- 6 I. Kuznetsova, T. Meier, S. T. Cundiff, and P. Thomas, *Phys. Rev. B* **76**, 153301 (2007).
- 7 L. Yang, I. V. Schweigert, S. T. Cundiff and S. Mukamel, *Phys. Rev. B* **75**, 125302 (2007).
- 8 K. W. Stone, K. Gundogdu, D. B. Turner, K. A. Nelson, X. Li, and S. T. Cundiff, "Two-quantum 2D optical FT spectroscopy of biexcitons in GaAs quantum wells," submitted for publication.
- 9 G. S. Engel, T. R. Calhoun, E. L. Read, T.-K. Ahn, T. Mančal, Y.-C. Cheng, R. E. Blankenship and G. R. Fleming, *Nature* **446**, 782 (2007).